frontiers | Frontiers in Industrial Microbiology

TYPE Original Research
PUBLISHED 23 July 2024
DOI 10.3389/finmi.2024.1426067

OPEN ACCESS

EDITED BY
Vanja Jurisic,
University of Zagreb, Croatia

REVIEWED BY
Mark Mba Wright,
Iowa State University, United States
Shraddha Maitra,
University of Illinois at Urbana-Champaign, United States

*CORRESPONDENCE
Ethan Struhs
estruhs@uidaho.edu
Amin Mirkouei
amirkouei@uidaho.edu

RECEIVED 30 April 2024
ACCEPTED 01 July 2024
PUBLISHED 23 July 2024

CITATION
Struhs E, Mirkouei A, Appiah H and McDonald AG (2024) Examination of *in situ* and *ex situ* catalytic fast pyrolysis and liquid fractionation utilizing a free-fall reactor. *Front. Ind. Microbiol.* 2:1426067. doi: 10.3389/finmi.2024.1426067

Examination of *in situ* and *ex situ* catalytic fast pyrolysis and liquid fractionation utilizing a free-fall reactor

Ethan Struhs[1]*, Amin Mirkouei[1,2]*, Harrison Appiah[3] and Armando G. McDonald[3]

[1]Department of Mechanical Engineering, University of Idaho, Idaho Falls, ID, United States, [2]Department of Nuclear Engineering and Industrial Management, University of Idaho, Idaho Falls, ID, United States, [3]Department of Forest, Rangeland and Fire Sciences, University of Idaho, Moscow, ID, United States

This study examines biomass valorization through thermochemical conversion by an integrated catalytic fast pyrolysis process with liquid fractionation using a free-fall reactor, γ-alumina, as a catalyst and methanol for direct quenching. The novelty lies within the process intensification (i.e., a single-step conversion and fractionation pathway) to improve pyrolysis oil yield and quality. In particular, the conversion bioprocess utilizes *in situ* or *ex situ* catalytic free-fall fast pyrolysis reactors at 550°C and 10–15 psi to produce pyrolysis oil and char (bio-oil and biochar) from pinewood feedstocks. The results from the gas chromatography–mass spectrometry show that the main volatile fractions of bio-oil compounds are levoglucosan, furfural, hydroxy acetone, methyl acetate, and catechol. The electrospray ionization–mass spectrometry results determine the average molar mass, revealing improved cracking, thermal treatment, and fraction stabilization. The Fourier transform infrared spectroscopy and thermal aging provide insight into the change in functional groups in relation to experimental parameters. The outcomes indicate that γ-alumina successfully decreased acidic compounds and increased esters and phenolic content in the bio-oil. The bio-oil produced from the *ex situ* catalytic pyrolysis also shows the highest liquid yield (~41%), high phenolic content, and thermally stable properties. The *in situ* catalytic pyrolysis exhibits lower yields but favors high ketone formation. Fractions condensed in methanol exhibit the highest thermal stability and esterification potential; however, they still possess relatively high amounts of acidic compounds. It is concluded that *ex situ* catalytic pyrolysis, using γ-alumina catalyst and fractionation with methanol, can improve conversion reactions, particularly bio-oil quality, yield, and thermal stability.

KEYWORDS

biomass, bio-oil, catalytic pyrolysis, characterization, thermochemical conversion, thermal stability

1 Introduction

Among renewable energy sources in the United States (US), biomass contributed the largest portion (38%) to bioenergy production in 2022 (U.S. DOE Energy Information Administration, 2023). Producing renewable energy using available renewable resources (e.g., biomass feedstocks) is a promising alternative to offset reliance on non-renewable resources (e.g., fossil fuels) (Myllyviita et al., 2012). Many conversion processes can provide potential routes for converting raw biomass to chemicals, heat, fuels, and power (Alizadeh et al., 2020). However, the costs of current technologies for biomass pretreatment, conversion, and upgrading make biofuel production economically impractical (Mirkouei et al., 2017). Evaluating biomass conversion pathway technologies is critical to identifying optimal processes and producing valorized energy products (Venderbosch, 2015). Of these processes, thermochemical decomposition of biomass by fast pyrolysis (FP) has shown to be simple and comparatively cost-effective in producing a liquid product with higher energy content than the raw materials (Mirkouei et al., 2016). Pyrolysis-oil (often called "bio-oil") is the liquid product from the pyrolysis of lignocellulosic materials that can be used as a heating source in its raw form (Easterly, 2002). Conversely, some of bio-oil's quality attributes, such as low heating value, corrosivity, and thermal instability, make it inequivalent to existing petroleum-based transportation fuels (e.g., gasoline and diesel). The lower heating value of bio-oil is associated with the high oxygen and water content as well as the low hydrogen-to-carbon (H/C) ratio and high oxygen-to-carbon (O/C) ratio (Jacobson et al., 2013). Some other unwanted bio-oil characteristics (e.g., viscosity and acidity) preclude many other potential applications as well (Ramirez-Corredores and Sanchez, 2012). Biofuels and bio-blendstocks produced from bio-oils have been considered as a potential source of renewable transportation fuels (Li et al., 2015). However, the corrosivity of an acidic fuel ruins boiler, turbines, and engine components (Brady et al., 2014), while storage and thermal instability limit processing and prevent long-term storage necessary for distribution at the commercial level (Yang et al., 2015). Therefore, upgrading treatments (before storage and distribution) attempts to address bio-oil quality issues and improve usability and applicability.

The addition of catalysts to the pyrolysis process improves key chemical reactions, such as cracking, hydrogenation, decarbonylation, and decarboxylation (Zhang et al., 2007). Furthermore, the addition of hydrogen gas with catalyst can lead to hydrocracking, hydrogenation, and hydrodeoxygenation (Fermoso et al., 2017). The goal of catalysis is to produce a bio-oil with fewer oxygenated compounds and increased hydrocarbon and short chain molecule content. Solid acid catalysts (e.g., zeolite) have been shown to possess superior cracking and dehydration activity, making them preferable for catalytic pyrolysis (Dickerson and Soria, 2013). However, due to the microporous structure and acidity of zeolite, pore blockage from polymerization and polycondensation reactions results in a low bio-oil yield and rapid catalyst deactivation from coke formation (Imran et al., 2018). While not as effective as zeolites, other catalysts have merit in being used for catalytic pyrolysis, such as γ-alumina, due to lower costs and desirable characteristics (i.e., surface area, pore volume, and pore size distribution) (Trueba and Trasatti, 2005). γ-Alumina is a solid acid catalyst and exhibits high activity due to a large number of Lewis acid sites on its surface (Mosallanejad et al., 2018). The effectiveness of γ-alumina can also be increased by using it as a catalyst support. Depending on the results of the bio-oil composition, undesirable functional groups for fuel product may be identified and targeted in further experiments by decorating the γ-alumina with metals (e.g., Ni, Mo, Co, and Fe), increasing active sites for cracking and reforming reactions (Zhang et al., 2018). Gupta and Mondal (2021) performed pyrolysis on pine needles using γ-alumina and nickel-doped γ-alumina (Gupta and Mondal, 2021). The results showed that the catalyst caused a considerable reduction in activation energy and improved reaction rate. The catalyst also increased the phenolic content in the bio-oil and reduced the oxygen content. Other studies have shown that using reactive distillation with an alcohol and an acid catalyst resulted in bio-oil esterification and improved fuel qualities (Mahfud et al., 2007; Junming et al., 2008).

Another technique that can be integrated into a pyrolysis unit to increase bio-oil yield and quality is the utilization of direct quenching columns (e.g., spray towers and impingers). Pyrolysis units commonly utilize these columns due to the physical and chemical condensation interactions between the quenching fluid and pyrolysis vapors. Condensation achieved in this way can capture lighter-weight molecules and mitigate undesirable reactions (Bridgwater, 2012). Earlier studies investigated various quenching fluids, such as water (Vasalos et al., 2016), paraffin oil (Park et al., 2016), liquid nitrogen (Dalluge et al., 2019), reused bio-oil (Cai and Liu, 2016), immiscible hydrocarbon solvents (Papari and Hawboldt, 2018), alcohols (Dufour et al., 2007), and dichloromethane (Sotoudehnia et al., 2021). Methanol is particularly interesting since it is relatively inexpensive and very effective at decreasing the aging rate of bio-oil (Diebold and Czernik, 1997; Oasmaa et al., 2004; Wenting et al., 2014). Suggested reactions that occur between bio-oil compounds and methanol include esterification and acetalization, resulting in a simple, economically feasible upgrading approach (Oasmaa and Czernik, 1999).

This research utilizes a free-fall reactor configuration for the fast pyrolysis of pinewood particles. The rationales behind the free-fall pyrolysis reactor lie in the simple conversion pathway design, efficient control, high liquid yield, and minimal use of sweep gas as well as convenient control of the kinetic parameters, mass balance, and residence time (Lehto, 2007; Ellens and Brown, 2012; Punsuwan and Tangsathitkulchai, 2014). The focus of this research is on evaluating the effect of *in situ* and *ex situ* free-fall catalytic fast pyrolysis (CFP). While CFP is commonly practiced, to the best of our knowledge, there is no study on a free-fall CFP reactor. This study also integrates a direct quenching column in the form of a methanol impinger to both increase the bio-oil yield capture and assess the quenching fluid's effects on condensed products. Comparisons of liquid fractions will be made to a previous study utilizing the same reactor (Struhs et al., 2022). Table 1 presents an overview of earlier similar studies and the main differences between them and this study.

This study proposes a mixed catalytic fast pyrolysis process with liquid fractionation using a free-fall reactor, γ-alumina, as a catalyst and methanol for direct quenching. The novelty lies within the process intensification, a single-step conversion and fractionation pathway, to improve pyrolysis oil yield and quality. This study compares the advantages and deficiencies of the proposed conversion pathways with prior studies, along with the potential of γ-alumina in CFP, and the efficiency and effect of methanol as a direct quenching fluid. This study attempts to address stable bio-oil production from biomass and improve usability and applicability. To do so, the effectiveness of *ex situ* and *in situ* CFP is examined and compared. The physicochemical properties of methanol as a quenching fluid and stabilizing agent are also assessed. The key research impacts of this study are as follows: (a) assisting in defining the basic principles that guide the production of stable bio-oil and (b) explaining the resulting phenomena occurring in the catalysis and direct quenching of pyrolysis vapors.

2 Materials and methods

2.1 Materials

Biomass: Pinewood flour (PWF) was used as the sole biomass feedstock in this study, sourced from American Wood Fibers (Table 2). PWF was dried to a moisture content of below 10% and screened (between 60 and 120 standard mesh) to a particle size between 125 and 250 μm. The moisture content of the feedstock was accounted for by mass difference before and after drying in the oven at 105°C for 12 h.

Catalyst: The catalyst used in this study has a hollow cylinder (Raschig ring) structure and is composed of γ-alumina (GH New Material). This structure was chosen to eliminate char blockage when performing in situ catalysis. The γ-alumina possessed a BET surface area of 231 m^2/g and pore volume of 0.66 cm^3/g.

TABLE 1 Recent pyrolysis studies utilizing γ-alumina and/or direct quenching methods.

Study	Catalyst		Condensing method	Reactor	Feedstock	Focus	Benefits
Matsuoka et al., 2006	γ-Al_2O_3	*In situ*	Cold trap	Fluidized bed	Oak sawdust	Water–gas shift reaction	Tar capture, high mechanical strength
Dufour et al., 2007	–	–	Methanol impinger, SPA tubes	Semi batch	Spruce chips	Condensing method effect on product	–
Quirino et al., 2009	$(SnO)_2(Al_2O_3)_8$, $(SnO)_1(ZnO)_1(Al_2O_3)$, $(ZnO)_2(Al_2O_3)_8$	*In situ*	Glass condenser	Semi batch	Soybean oil	Effects of catalyst on products' composition	Deoxygenating effects
Ateş and Işıkdağ, 2009	Al_2O_3	*In situ*	Ice bath	Semi batch	Corncob	Liquid composition, yields	Decreased reaction temperature and oxygenated compounds
Du et al., 2014	ZSM-5, Al_2O_3–SiO_2	*In situ*	Methanol impinger	Spouted bed reactor	Miscanthus	Operating conditions, product distribution	Monocyclic aromatic hydrocarbons production, activity
Chen et al., 2017	ZSM-5, γ-Al_2O_3	*In situ*	Impinger	Semi batch	Castor meal	Effects of catalyst on products' composition	Decreased reaction temperature, enhanced secondary reactions, deoxygenation, decreased liquid viscosity
Jia et al., 2017	H-ZSM-5 and derivative	*In situ*	Cold trap, propanol N_2 impinger	Micro-fluidized bed reactor	Oak sawdust	Effect of different zeolite catalysts on products	Increased selectivity of monoaromatics
Ghorbannezhad et al., 2020	Na_2CO_3/γ-Al_2O_3, HZSM-5	*Ex situ*	–	Tandem microreactor	Sugarcane bagasse/PET	Effects of catalyst on products' composition	Deoxygenation, reduced coke formation
Gupta and Mondal, 2021	γ-Al_2O_3, Ni/γ-Al_2O_3	*In situ*	Water/ice baths	Semi batch	Pine needles	Thermal degradation, kinetics	Reduced activation energy, increased rection rate, deoxygenation
This study	γ-Al_2O_3	*In situ*, *ex situ*	Shell and tube/ methanol impinger	Continuous free-fall reactor	Pinewood particles	Effects of catalyst on product composition, process configuration	

TABLE 2 Characterization of raw PWF (US Department of Energy, Idaho National Laboratory, 2016).

Feedstock	Volatile matter (%)	Ash (%)	Fixed carbon (%)	Moisture content (%)	Particle size (μm)
Pine	84.50 ± 4.23	1.08 ± 0.05	14.41 ± 0.72	7.3 ± 0.37	125–250

Experimental setup: The thermochemical conversion of pinewood was achieved using a free-fall fast pyrolysis reactor (Figure 1). The free-fall reactor is a gas–solid co-current downflow cylindrical reactor (inner diameter of 2.09 cm and length of 107 cm). Biomass was continuously fed into the reactor using a motorized auger feed system, located at the top of the reactor, at 10 g/min over a span of 5 min. The system pressure was monitored and varied between 0 and 48 kPa_g. Temperature was set at 550°C with an approximated biomass residence time of 0.7–1 s. The reactor was heated using external tape heaters and an internal heating cartridge, which were controlled using programmable logic controllers. Thermocouples were attached to the reactor wall and the heating cartridge to monitor temperature at multiple points along the unit. For *in situ* catalytic fast pyrolysis (I-CFP), a catalyst bed was placed in the bottom of the free-fall reactor, giving the biomass sufficient time to pyrolyze before the vapors and char passed through the catalyst. A catalyst bed was placed directly after the cyclone for *ex situ* catalytic fast pyrolysis (E-CFP). Our previous experiments performed on PWF used the free-fall reactor without incorporating catalysts or direct quenching (Struhs et al., 2022).

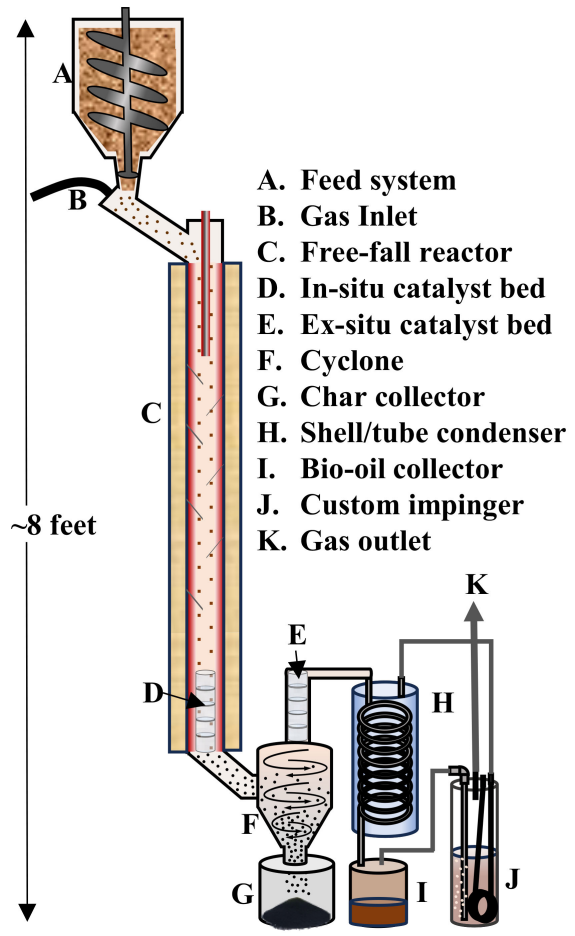

FIGURE 1
Diagram of CFP reactor unit used for pyrolysis experiments.

The solid biochar was separated from the pyrolysis vapors via a cyclone. A custom impinger-type direct quencher was fabricated and placed in series with a shell and tube condenser directly after the cyclone. For the catalytic experiments, the impinger was placed after the shell and tube condenser. Additional experiments were performed where the impinger was placed first in series (FPQ) to examine the effect on bio-oil fractions; however, no catalyst was used in these experiments. The indirect condenser was cooled using a chiller filled with a mix of water and ethylene glycol at 0°C. The pyrolysis vapors were rapidly cooled and condensed by the impinger using a known amount of methanol (100 mL) kept at 0°C by internal coils connected to the chiller. Bio-oil fractions were condensed inside both columns and analyzed separately. After the experiment, the bio-oil and methanol were collected and stored in a refrigerator at 5°C to mitigate the change in composition due to potential bio-oil instability. Bio-oil and char yield were determined gravimetrically, and gas was calculated by difference. The experiments under different conditions were performed in triplicate.

2.2 Product characterization

Bio-oil samples were characterized using bomb calorimetry, gas chromatography–mass spectrometry (GC–MS), electrospray ionization–mass spectrometry (ESI–MS), Fourier transform infrared (FTIR), and thermal stability aging as well as proximate analysis for biochar characterization as detailed below:

Proximate analysis: Higher heating values (HHV) of the biochar and bio-oil (dried over anhydrous sodium sulfate prior to analysis) samples were obtained by bomb calorimetry (Parr Instruments model 1261) according to ASTM D5865-04 and calibrated with benzoic acid.

GC–MS: The semi-volatile composition of the bio-oil was determined by GC–MS analyses and carried out in duplicate (Trace 1300-ISQ, ThermoScientific). GC–MS samples were prepared by mixing 1 mg bio-oil with 1 mL CH_2Cl_2 containing trichlorobenzene (100 μg/mL) as an internal standard. A ZB-5 capillary column (30 m × 0.25 mm, Phenomenex) was used to separate the bio-oil compounds using a temperature program of 40°C (1 min) to 250°C (10 min) at 5°C/min and an injector temperature of 255°C. Peaks on the chromatogram were identified using authentic standards from the literature and the NIST 2017 MS library (Faix et al., 1990a, b, 1991).

ESI–MS: Molar mass, monomer/oligomer ratios, and predominant compounds of the bio-oil samples were determined using spectral mass distribution obtained from a Finnigan LCQ-Deca mass spectrometer (ThermoQuest) (Sotoudehnia et al., 2020).

The ESI–MS samples were made by dissolving bio-oil (1 mg/mL) in 99% methanol/1% acetic acid solution before being injected and exposed to negative ion ESI–MS (m/z 100–2,000) at a flow rate of 10 µL/min. The temperature was set to 275°C, with capillary and ion source voltages set to 4.5 kV and 50 V, respectively. Equations 1 and 2 were used to calculate the molar masses as the number-average (M_n) and weight-average (M_w), where N_i is the intensity of ions and M_i is the ion mass (Sotoudehniakarani et al., 2019; Sotoudehnia et al., 2020).

$$M_n = \sum N_i M_i / \sum N_i \quad (1)$$

$$M_w = \sum N_i M_i^2 / \sum N_i M_i \quad (2)$$

FTIR: Major functional groups and compounds were identified by FTIR spectra of bio-oil samples. Spectra were obtained in duplicate using a ZnSe-attenuated total reflection (iD5 ATR) accessory of a Thermo-Nicolet iS5 spectrometer. The (Thermo-Nicolet) Omnic v9 software was used for baseline correction, averaging the FTIR spectra, and for identifying functional group frequencies.

Thermal stability: The thermal stability test was performed by rapidly aging the bio-oil at a moderate temperature and measuring the change in viscosity (NDJ-9S viscometer, spindle 2 at 60 rpm) over time. When undergoing accelerated aging, bio-oil shows a decrease in total molecules but an increase in molecular weight, indicating condensation reactions and water formation (Oasmaa and Kuoppala, 2003; Elliott et al., 2012). Methods for the thermal stability test and obtaining the stability parameter (SP) can be found in our previously published study (Struhs et al., 2022). Equation 3 was used to calculate the SP values:

$$SP = \frac{\partial\,(\text{Viscosity})}{\partial\,(\text{time})}\ cp/h \quad (3)$$

3 Results and discussion

3.1 Product yield results

Bio-oil yield is represented by the average and standard deviation of the sum of oil collected from the condenser and impinger over three experiments. Table 3 shows the yields of products collected.

I-CFP resulted in higher solids (char and coke) and gas yields than E-CFP, while *ex situ* had higher liquid yields. Through a *t*-test, it was found that the difference in the means of liquid yield barely fails to reject the null hypothesis (p = 0.05). Without a moisture content measurement, the significance of the quality of the yield difference is also hard to determine. Prior comparison studies of *in situ* and *ex situ* pyrolysis generally find higher liquid yields from *ex situ* pyrolysis (Wang et al., 2014; Luo and Resende, 2016). Earlier published studies examining free-fall FP reveal yields of 35–45% for bio-oil, though none incorporates a catalyst (Li et al., 2004; Pattiya et al., 2012; Ngo and Kim, 2014). Other studies that looked into the catalytic effects of γ-alumina revealed liquid yields between 22% and 49% (Ateş and Işıkdağ, 2009; Chen et al., 2017; Gupta and Mondal, 2021). Liquid yields were higher and solid yields were lower in comparison to data produced for pyrolysis of PWF with no catalyst, which may be attributed to an increase in heat transfer efficiency inside the reactor and the incorporation of the impinger. The impinger was responsible for capturing 6%–14% of the total bio-oil yield during catalytic pyrolysis experiments. Further bio-oil yields could potentially be achieved through reducing char and gas byproducts by increasing the operating temperature, minimizing the initial biomass moisture content, and increasing the biomass heating rates (Akhtar and Saidina Amin, 2012).

TABLE 3 Liquid yield of free-fall FP from different reactor configurations.

Process	Bio-oil (%)
FP	23.3 ± 1.2
E-CFP	41.1 ± 4.3
I-CFP	31.9 ± 1.5
FPQ	38.5 ± 3.2

FP, fast pyrolysis; E-CFP, *ex situ* catalytic pyrolysis; I-CFP, *in situ* catalytic pyrolysis; FPQ, fast pyrolysis with direct quenching.

3.2 Bio-oil heating value results

HHV values fall within 16–23 MJ/kg found for other bio-oil samples in prior studies with the exception of I-CFP (Kang et al., 2006; Hassan et al., 2009). Figure 2 compares the HHV of commercial fuels or solvents with liquid samples collected in this study. FPQ produced bio-oils with the highest HHV, close to that of methanol. Physicochemical interactions during the condensation of vapors may contribute to this result. Traces of methanol may also have evaporated and recondensed in the second condenser. I-CFP samples performed the worst, indicating undesirable cracking reactions when considering product fuel quality. The addition of 10 wt% methanol increased the HHV for E-CFP samples by an average of 17% while showing a slight change in FPQ samples. An insufficient I-CFP sample led to inconclusive results when adding methanol. Still the HHV of the samples falls well short of

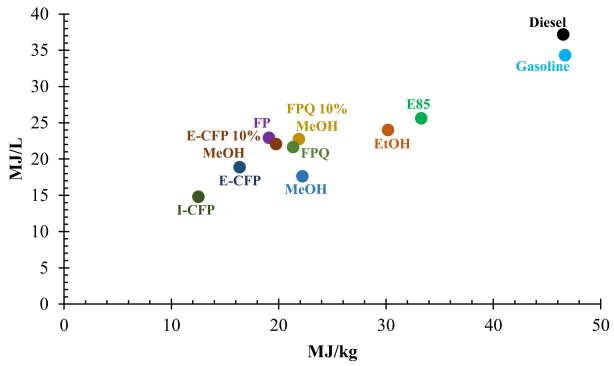

FIGURE 2
Energy densities of bio-oil samples compared with commercial fuels and solvents.

conventional fuels by 40%–50% due to the large presence of oxygenated compounds. This is generally the case with biomass-derived bio-oil and can be remedied through post-processing of the pyrolysis liquid. While heating value alone would not be enough to determine the fuel blending potential, further treatment of bio-oil (e.g., fluid catalytic cracking, hydrotreating, distillation, and electrochemical) would be required if a pathway for fuel production was desired (Zhang et al., 2007). Such treatment processes have been used to decrease the energy density gap and produce biofuels (Botella et al., 2018; Hita et al., 2020).

3.3 Bio-oil thermal stability results

The results of bio-oil viscosity show a relative linear correlation, given by R^2 values close to 1 (Figure 3).

The initial viscosities before the addition of alcohol ranged between 20 and 30 cP. The SP values were determined using data obtained from the thermal aging experiments and ranged between 0.1 and 0.2 cP/h for methanol-added bio-oils and between 0.7 and 1.3 cP/h for the bio-oils (Table 4). Other stability studies covering the addition of methanol give SP values from 0.5 to 11 cP/h, backing the results of this study (Czernik et al., 1994; Oasmaa and Kuoppala, 2003). Methanol addition decreased the viscosity and reduced the rate of increasing viscosity of bio-oils. Bio-oils produced during E-CFP had slightly higher initial viscosities and SP values, while those produced from FPQ had both the lowest initial viscosities and SP values. The low viscosity values for the FPQ samples could be attributed to a decrease in acidic compounds due to the catalytic effects of γ-alumina (Trueba and Trasatti, 2005). The FPQ liquid samples were collected in the second condenser following the impinger, resulting in a bio-oil that shows the least change in viscosity over time. This could be the result of some interaction with the vapor initially passing through the methanol or trace amounts of methanol vaporizing and condensing in the second condenser, increasing the stability of the fraction (Diebold and Czernik, 1997). Viscosity increases show that the addition of solvent does not completely stop thermal degradation and that condensation reactions still occur. Studies show that long-term storage of blends could potentially decrease viscosity and total acid number, but with an increase in water content (Zhang and Wu, 2014). Blending could be a short-term stabilization and storage solution before further catalytic upgrading. Further characterization analysis during each step of the aging process would be beneficial in determining the specific stabilizing reactions and the impact on functional groups. The SP results show that the use of γ-alumina as a catalyst for fast pyrolysis has a significant positive effect on bio-oil stability.

3.4 Gas chromatography–mass spectrometry results

3.4.1 Shell and tube condenser

GC–MS was used to examine the volatile compounds in the bio-oil produced by the different pyrolysis unit configurations (Figure 4) (Khuenkaeo and Tippayawong, 2020; Zhang et al., 2021).

Chemical compounds identified in the chromatograms were diverse in structure (e.g., phenolics, sugar derivatives, furans, ketones, alcohols, aldehydes, and acids), with carbon atoms ranging from C_2 to C_{20} (Lyu et al., 2015). The results show a high amount of phenolic compounds with methoxy-substitutes and benzenediols phenols, which are attributed to high amounts of guaiacyl and syringyl units in the lignin fraction of PWF (Poletto, 2018). The presence of syringyl units is likely from hardwood species present in the PWF. The complexity and variety of phenolics indicate that recombination reactions occurred among intermediates after primary decomposition reactions.

Levoglucosan is the primary compound in the E-CFP and FPQ bio-oil samples while also being predominant in I-CFP samples (Table 5). I-CFP seemed to favor the production of ketones, namely, hydroxy acetone. This results from the cracking of anhydro-sugars by dehydration and decarbonylation reactions favored in the I-CFP configuration (Hu et al., 2019). It is also speculated that a longer residence time caused by the integration of a catalyst bed in the reactor and a low feed/gas flow rate contributed to the ketonization of carboxylic acids, producing ketones, water, and carbon dioxide (Isahak et al., 2012; Pham et al., 2013). The additional water

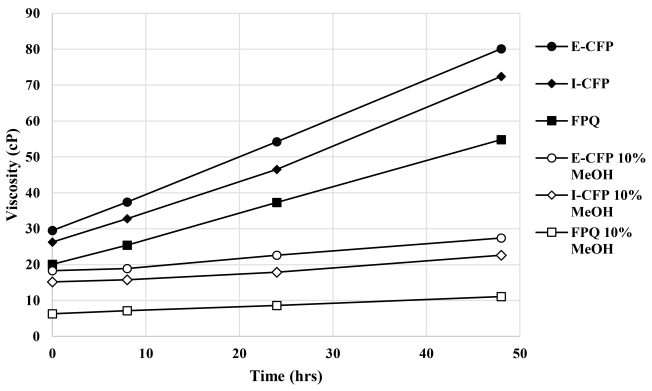

FIGURE 3
Bio-oil viscosity changes over time.

TABLE 4 SP values for bio-oil samples.

	FP	E-CFP	I-CFP	FPQ	E-CFP 10% MeOH	I-CFP 10% MeOH	FPQ 10% MeOH
SP (cP/h)	1.33	1.06	0.96	0.73	0.20	0.16	0.10
R^2	0.98	0.99	0.99	0.99	0.99	0.98	0.99

formation could explain the decrease in HHV for the I-CFP samples examined earlier.

Figure 5 reveals the relative abundance of functional groups among the volatile compounds identified through GC–MS. I-CFP and E-CFP samples show a slightly decreased content of sugar-derived compounds caused by the catalyst via decarbonylation, decarboxylation, dehydration, and cracking reactions, leading to the formation of alcohols, furans, and ketones. These compounds then can also undergo further conversion, resulting in phenols (Hu et al., 2022). There is only a small change in alcohol, aldehyde, furan, and ketone content after catalytic reactions in E-CFP due to the secondary reactions. E-CFP samples have the highest phenolic content. This can be attributed to the cracking properties of the catalyst transforming lignin-derived compounds into phenols through the cleavage of C–O and C–C bonds (Hu et al., 2022). Lewis acid sites on the surface of the catalyst also allow for rehydroxylation reactions, permitting water to be converted into hydroxy groups (Trueba and Trasatti, 2005). FPQ samples also exhibited high amounts of phenolic content. With no catalyst used, it is assumed that the methanol reacted with the pyrolysis vapors, increasing alkylated phenols and aromatics (Horne et al., 1995). Methanol also shows a stabilizing effect on the second fraction, resulting in fewer condensation reactions and leading to a higher content of lighter molecules. The phenolic content in bio-oil has industrial significance for resin, adhesive, dye, pharmaceutical, and food additive production (Kim and Park, 2020). Other studies showed that the use of γ-alumina significantly increases the amount of phenol and phenolics (Chen et al., 2017; Gupta and Mondal, 2021). Appropriate analysis and extraction

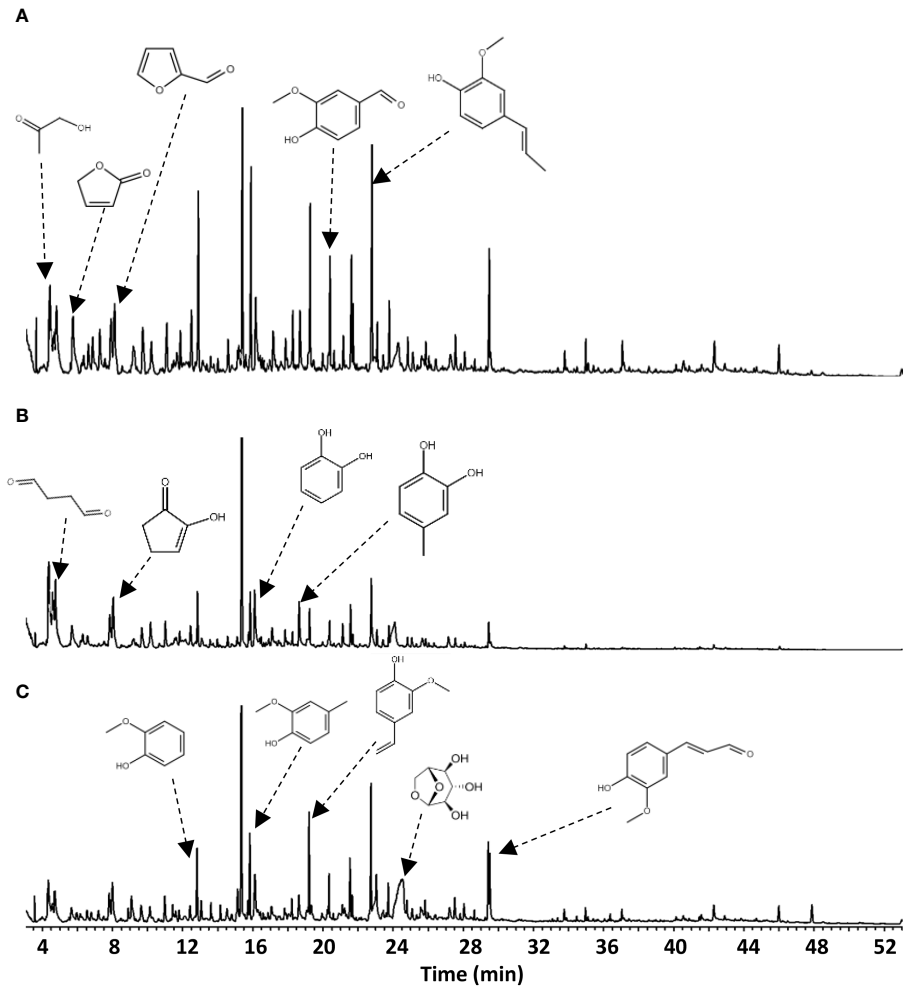

FIGURE 4
GC–MS chromatograms of bio-oil collected from **(A)** E-CFP, **(B)** I-CFP, and **(C)** FPQ experiments.

10.3389/finmi.2024.1426067

TABLE 5 High-concentration compounds identified by GC–MS in bio-oil samples.

Compound	M+	Formula	Residence time	FP	E-CFP	I-CFP	FPQ
				µg/mg			
Acetic acid	60	$C_2H_4O_2$	3.67	4.44	–	–	–
Hydroxyacetone	74	$C_3H_6O_2$	4.33	0.35	5.13	9.36	6.37
Succindialdehyde	86	C_4H6O_2	4.56	0.76	2.53	4.43	1.48
Dihydro-4-hydroxy-2(3H)-furanone	102	C_4H6O_3	4.71	–	3.40	4.03	–
3-Methyl-butanal	86	$C_5H_{10}O$	4.83	1.06	–	–	–
Furfural	96	$C_5H_4O_2$	5.65	3.62	2.62	1.52	1.32
Tetrahydro-2,5-dimethoxy-furan	132	$C_6H_{12}O_3$	7.19	0.32	2.45	0.98	2.50
2(5H)-Furanone	84	$C_4H_4O_2$	7.81	2.43	2.56	2.14	2.17
2-Hydroxy-2-cyclopenten-1-one	98	$C_5H_6O_2$	8.00	1.81	3.82	2.74	3.78
2-Methyl-1,2-hexanediol	132	$C_7H_{16}O_2$	9.08	–	–	2.17	–
Phenol	94	C_6H_6O	9.63	1.36	1.85	1.01	1.57
3-Methyl-1,2-cyclopentanedione	112	$C_6H_8O_2$	10.99	1.3	1.49	1.10	1.60
Guaiacol	124	$C_7H_8O_2$	12.81	2.78	3.34	1.81	3.77
1,2-Cyclopentanediol	102	$C_5H_{10}O_2$	13.03	–	–	0.86	1.08
Creosol	138	$C_8H_{10}O_2$	15.82	2.6	3.20	1.62	4.15
Catechol	110	$C_6H_6O_2$	16.07	1.94	3.49	2.38	4.69
1,4:3,6-Dianhydro-α-d-glucopyranose	144	$C_6H_8O_4$	16.37	–	0.32	0.83	–
5-Hydroxymethylfurfural	126	$C_6H_6O_3$	17.10	0.53	1.07	0.76	1.54
4-Methylcatechol	124	$C_7H_8O_2$	18.60	1.62	2.79	1.57	2.73
Vinyl guaiacol	150	$C_9H_{10}O_2$	19.20	0.34	2.61	1.31	0.45
Eugenol	164	$C_{10}H_{12}O_2$	20.34	1.05	1.64	1.76	2.12
Geraniol	154	$C_{10}H_{18}O$	21.18	–	–	0.62	0.56
Vanillin	152	$C_8H_8O_3$	21.53	2.43	2.51	1.16	2.77
Isoeugenol	164	$C_{10}H_{12}O_2$	22.73	4.48	6.25	2.25	6.49
Propyl-guaiacol	166	$C_{10}H_{14}O_2$	23.04	0.36	0.84	0.25	4.17
Methyl syringol	168	$C_9H_{12}O_3$	23.06	2.8	–	–	–
Apocynin	166	$C_9H_{10}O_3$	23.71	–	1.29	1.44	–
Levoglucosan	162	$C_6H_{10}O_5$	24.31	13.2	8.57	5.05	15.99
Syringaldehyde	182	$C_9H_{10}O_4$	28.17	1.15	–	–	–
Coniferyl aldehyde	178	$C_{10}H_{10}O_3$	29.41	–	2.28	0.70	8.19
Acetosyringone	196	$C_{10}H_{12}O_4$	29.77	2.93	–	–	–
5-Hydroxy-7-methoxyflavanone	270	$C_{16}H_{14}O_4$	42.11	1.17	–	–	–

The – symbol is to facilitate that the compound was not detected in the sample.

techniques (e.g., solvent extraction, column chromatography, and distillation) should be examined to pursue this application pathway (Kim, 2015; Mantilla et al., 2015). Both E-CFP and I-CFP showed a noticeable decrease in acidic compounds, leading to reduced corrosivity and improved thermal stability, as shown previously. All configurations resulted in a certain amount of ester formation, particularly FPQ, where the interaction between organic acids and alcohols produces esters (Grioui et al., 2014). It has been reported that the ester reactions during pyrolysis of biomass are promoted by acidic catalysts, such as γ-alumina (Zhang et al., 2006). These catalysts convert acidic compounds into esters through catalytic esterification. FPQ samples had the highest amount of ester content. This can be

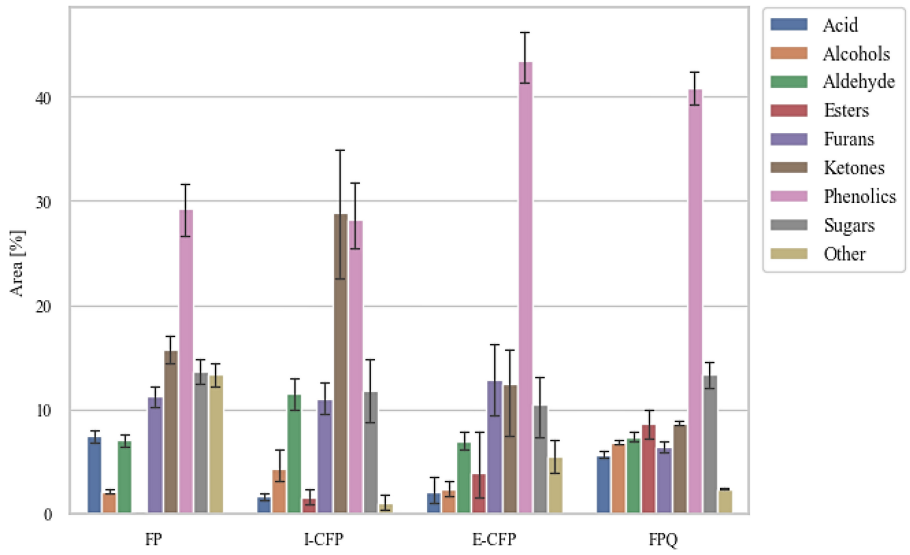

FIGURE 5
Abundance of functional groups identified in volatiles analyzed in bio-oil samples.

attributed to esterification that occurs when the vapors interact with the methanol in the impinger (Oasmaa and Czernik, 1999). FPQ still has relatively the same acid content as noncatalytic pyrolysis, emphasizing the effect γ-alumina has on acid conversion.

Fewer samples were captured in the methanol impingers during catalytic pyrolysis. Prominent compounds included oleic acid, methyl palmitate, glyceraldehyde, dodecyl acrylate, and other methyl esters. As the impinger was used as the primary condenser during FPQ, the compounds are more diverse but similar to the first fractions condensed during the catalytic experiments. Esterification of acids is recognized by the high presence of methyl acetate and isobutyl propionate (Liu et al., 2006). However, the carboxylic acid content was still high with the presence of pyruvic acid and higher-molecular-weight acids (e.g., homovanillic acid, 2-undecenoic acid, 9-hexadecenoic acid, and oleic acid) mostly found in the second bio-oil fraction.

3.5 Electrospray ionization–mass spectrometry results

ESI–MS analysis was used to determine the molar mass distribution of bio-oil (Figure 6) (Sotoudehniakarani et al., 2019; Sotoudehnia et al., 2020). Peaks generally spanned over the *m*/*z* range of 100–1,200 (Jarvis et al., 2012; Miettinen et al., 2015, 2017). The more noticeable $[M\text{-}H]^-$ ions were credited at *m*/*z* 161 to levoglucosan, *m*/*z* 109 to catechol, *m*/*z* 123 to guaiacol, and *m*/*z* 123 to coniferyl aldehyde. Subfractions of lignin-derived compounds, such as anhydro-sugars and phenolics, appear as peaks between *m*/*z* 300 and 350 (Jarvis et al., 2012; Liu et al., 2012; Miettinen et al., 2015). The GC–MS results verify the volatile compounds identified. Further mass analysis and equivalent homologue series are required to thoroughly identify compounds. Peaks produced through ESI–MS reveal higher-molecular-weight compounds than the volatiles identified by GC–MS, allowing for mass calculations.

Molar masses (M_w and M_n) of bio-oil samples were determined using prior studies on negative ion ESI–MS (Table 6). The spectra revealed bimodal distribution seen mostly in the condenser samples centered on *m*/*z* 250 and 450, indicating monomers and oligomers, respectively. Due to the bimodal distribution, the ion intensity ratio of *m*/*z* 100–300/*m*/*z* 301–2,000 was used to calculate the ratio of monomers to oligomers. The highest monomer/oligomer ratio belonged to fractions produced during FPQ, being significantly higher than any other sample and all methods being higher than FP, which indicates improved thermal breaking caused by both catalysis and direct quenching. Generally, because of thermal instability, bio-oil undergoes oligomerization during storage, resulting in the average molecular mass to increase between the time of pyrolysis and ESI–MS measurements. FPQ proved to have the best results because of methanol's stabilizing effects which decreased oligomerization. Earlier studies reported average molecular weights of around 300–800, complementing the results of this study (Liu et al., 2012; Harman-Ware et al., 2020). These results are also consistent with the thermal stability of the samples analyzed earlier. The most stable bio-oils in descending order were obtained during FPQ, I-CFP, E-CFP, and FP. I-CFP samples have the widest variance in molecular mass but ultimately seem very comparable in molecular weight to E-CFP. Samples collected in the second fraction tend to have lower molecular weights, proving the successful capture of some of the more volatile compounds that are entrained in the incondensable gas. Compared to FP, the effect of catalytic cracking seems to remedy the high average molecular weight and molar mass from previous experiments.

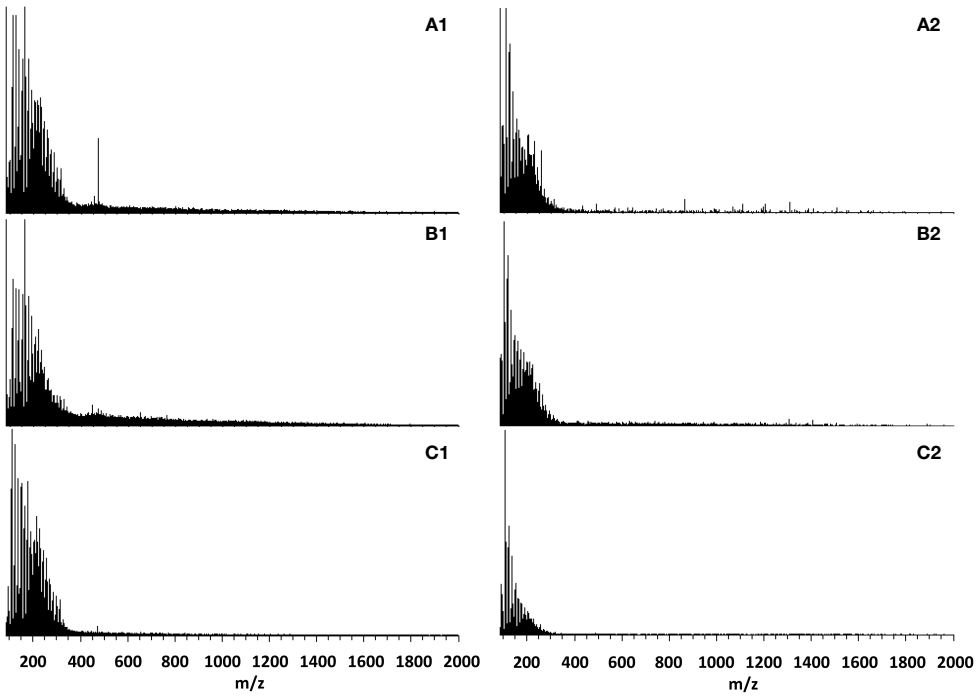

FIGURE 6
Negative-ion ESI–MS spectra of bio-oil produced from **(A1)** E-CFP condenser, **(A2)** E-CFP impinger, **(B1)** I-CFP condenser, **(B2)** I-CFP impinger, **(C1)** FPQ condenser, and **(C2)** FPQ impinger.

3.6 Fourier transform infrared spectroscopy results

FTIR analysis was used to verify the functional groups in the bio-oil samples (Figure 7).

Spectra were averaged taken for each experiment configuration and averaged before analysis. Band assignments for the bio-oils were acquired from the earlier published studies and labeled appropriately (Table 7) (Faix, 1992; Le et al., 2017). In the IR spectra, strong O–H stretching vibrations in all the samples around 3,365 cm^{-1} were indicative of phenols, acids, alcohols, and water (Cai et al., 2019). C–H stretching absorptions were seen at around 2,935 cm^{-1}, revealing the presence of possible aliphatic hydrocarbons (Xu et al., 2011). C=O stretching seen by absorption at 1,715 cm^{-1} suggests the presence of open-chain ketones and aryl aldehydes but was generally more suggestive of aliphatic and fatty acids (Tsai et al., 2006). At 1,515 cm^{-1}, the C=C–C stretching vibrations signify aromatics with various substitutions (Xu et al., 2018). Aromatic C–H and C–O stretching were related to the absorption at 1,032 cm^{-1}, revealing primary alcohols and guaiacyl compounds. At 813 cm^{-1}, aldehydes were identified by the aromatic C–H out of plane bending in lignin (Zhang et al., 2022). I-CFP seemed to have a prominent band at around 1,035 cm^{-1} relating to C–O and C–C–O of lignin and cellulose constituents (Chen et al., 2010). However, bands between 1,035 and 1,716 cm^{-1} were significantly lower than the other samples, showing lower C=C–C aromatic ring stretching and C–H bending and stretching. E-CFP has a noticeably large band at 1,716 cm^{-1}, which confirms the large number of phenolics/aromatics seen in the other

TABLE 6 Weight- (M_w) and number-average molar mass (M_n) of bio-oil samples determined from negative ion ESI–MS data.

Configuration	Fraction	M_n	M_w	Monomer/oligomer
FP	Condenser	564 ± 28	816 ± 41	0.45 ± 0.17
E-CFP	Condenser	387 ± 11	697 ± 20	1.66 ± 0.20
	Impinger	321 ± 117	603 ± 229	1.55 ± 0.94
I-CFP	Condenser	410 ± 61	726 ± 83	1.49 ± 0.92
	Impinger	514 ± 234	776 ± 292	0.56 ± 0.37
FPQ	Condenser	261 ± 10	453 ± 18	5.11 ± 0.89
	Impinger	264 ± 119	461 ± 199	5.06 ± 4.31

10.3389/finmi.2024.1426067

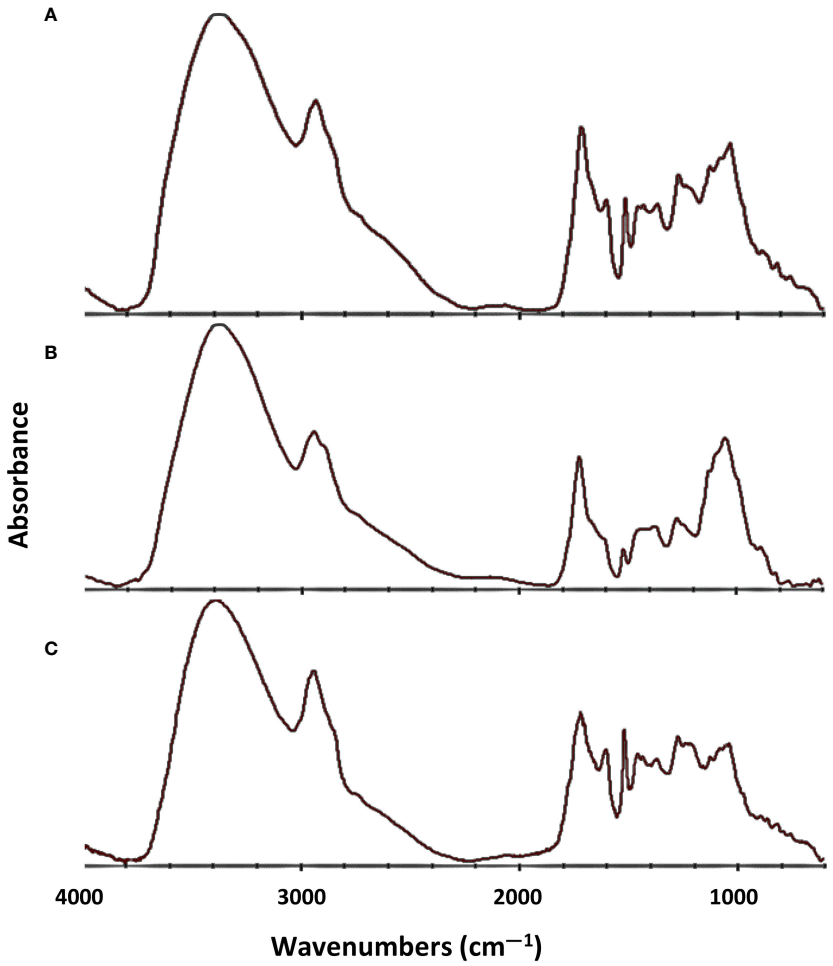

FIGURE 7
FTIR spectra of pyrolysis liquid collected from the condenser after **(A)** E-CFP, **(B)** I-CFP, and **(C)** FPQ.

TABLE 7 FTIR analysis results for E-CFP, I-CFP, and FPQ bio-oil samples.

Assignment/components	E-CFP	I-CFP	FPQ
O–H stretching (cellulose, hemicellulose, lignin)	3,359	3,367	3,374
C–H stretching (cellulose, hemicellulose, lignin)	2,930	2,935	2,936
C=O stretching (hemicellulose, lignin)	1,715	1,715	1,715
Aromatic skeletal vibration, C=O stretching, adsorbed O–H (hemicellulose, lignin)	1,597	1,604	1,597
C=C–C aromatic ring stretching and vibration (lignin)	1,514	1,515	1,514
C–H deformation (in methyl and methylene) (lignin)	1,454	1,429	1,454
C–H bending, C–H stretching in CH_3 (cellulose, hemicellulose, lignin)	1,362	1,362	1,362
H–C–H stretching methylene	1,268	1,268	1,270
C–O stretching of guaiacyl unit (lignin)	1,128	1,125	1,120
C–O stretching, aromatic C–H in plane deformation	1,032	1,035	1,032
–C–H bending vibration; aldehydes	883	878	888
Aromatic C–H out of plane bending (lignin)	813	813	813
C–H bending out of plane peaks (furfural)	755	753	755

(Continued)

analyses. The FTIR results for E-CFP show the greatest improvement in bio-oil quality compared to the other configurations. The overview of sample functionalization FTIR band and IR spectra provide a quick insight into chemical shifts that occur when changing experiment methodologies.

In order to better understand the valorization of biomass and improve the free-fall CFP conversion bioprocess, especially bio-oil quality and thermal stability, future studies can focus on the following directions:

- ➢ Exploration of several inexpensive hydrodeoxygenation catalysts in the *ex situ* CFP configuration.
- ➢ Examination of the effects of catalytic loading ratio and physical parameters on pyrolysis liquid product composition and yield.
- ➢ Exploration of direct quenching with varying solvents and their physicochemical effects on the liquid product.
- ➢ Investigation of solvent promoting fractionation and reactive distillation integrated with CFP.

4 Conclusion

The effects of γ-alumina as a catalyst for *in situ* and *ex situ* catalytic fast pyrolysis of pinewood in a customized free-fall reactor were successfully studied. The physicochemical effects of methanol as a direct quenching agent were also examined. All three pyrolysis process configurations had higher liquid and gas yields and greater thermal stability than the prior FP experiments. γ-Alumina had a significant positive effect on bio-oil thermal stability. The addition of 10 wt% methanol to samples improved the HHV by a visible amount. γ-Alumina, as an inexpensive catalyst support for hydrodeoxygenating catalysts (e.g., Ni, Mo, Fe, and Co), could remedy the insufficiencies of γ-alumina as a catalyst. Methanol was successful as a direct quenching agent for the first liquid fraction, converting much of the carboxylic acid content into fatty acid methyl esters, producing high phenolic content, and thermally stabilizing the fraction upon collection, resulting in a low-molecular-weight bio-oil fraction. The fraction did, however, still possess a visible amount of acidic compounds. The use of γ-alumina with methanol impingers for fractionation could potentially produce an oil high in small-chain esters and low in acids.

Data availability statement

The original contributions presented in the study are included in the article/supplementary material. Further inquiries can be directed to the corresponding authors.

Author contributions

ES: Conceptualization, Data curation, Formal analysis, Funding acquisition, Investigation, Methodology, Project administration, Resources, Software, Supervision, Validation, Visualization, Writing – original draft, Writing – review & editing. AMi: Conceptualization, Funding acquisition, Methodology, Project administration, Validation, Writing – original draft, Writing – review & editing. HA: Data curation, Formal analysis, Investigation, Resources, Software, Writing – original draft, Writing – review & editing. AMc: Conceptualization, Investigation, Methodology, Supervision, Validation, Writing – original draft, Writing – review & editing.

Funding

The author(s) declare financial support was received for the research, authorship, and/or publication of this article. The authors wish to acknowledge University of Idaho (UI) for Equipment and Infrastructure Support (EIS) awards and the United States Geological Survey (USGS) for 104b grant.

Acknowledgments

The authors wish to acknowledge American Wood Fibers for supplying biomass feedstocks as well as UI College of Natural Resources for providing the GC–MS, FTIR, and ESI–MS.

Conflict of interest

The authors declare that the research was conducted in the absence of any commercial or financial relationships that could be construed as a potential conflict of interest.

Publisher's note

References

Akhtar, J., and Saidina Amin, N. (2012). A review on operating parameters for optimum liquid oil yield in biomass pyrolysis. *Renewable Sustain. Energy Rev.* 16, 5101–5109. doi: 10.1016/j.rser.2012.05.033

Alizadeh, R., Lund, P. D., and Soltanisehat, L. (2020). Outlook on biofuels in future studies: A systematic literature review. *Renewable Sustain. Energy Rev.* 134, 110326. doi: 10.1016/j.rser.2020.110326

Ateş, F., and Işıkdağ, M. A. (2009). Influence of temperature and alumina catalyst on pyrolysis of corncob. *Fuel* 88, 1991–1997. doi: 10.1016/j.fuel.2009.03.008

Botella, L., Stankovikj, F., Sánchez, J. L., Gonzalo, A., Arauzo, J., and Garcia-Pérez, M. (2018). Bio-oil hydrotreatment for enhancing solubility in biodiesel and the oxydation stability of resulting blends. *Front. Chem.* 6. doi: 10.3389/fchem.2018.00083

Brady, M. P., Keiser, J. R., Leonard, D. N., Whitmer, L., and Thomson, J. K. (2014). Corrosion considerations for thermochemical biomass liquefaction process systems in biofuel production. *JOM* 66, 2583–2592. doi: 10.1007/s11837-014-1201-y

Bridgwater, A. V. (2012). Review of fast pyrolysis of biomass and product upgrading. *Biomass Bioenergy* 38, 68–94. doi: 10.1016/j.biombioe.2011.01.048

Cai, W., and Liu, R. (2016). Performance of a commercial-scale biomass fast pyrolysis plant for bio-oil production. *Fuel* 182, 677–686. doi: 10.1016/j.fuel.2016.06.030

Cai, W., Liu, Q., Shen, D., and Wang, J. (2019). Py-GC/MS analysis on product distribution of two-staged biomass pyrolysis. *J. Anal. Appl. Pyrol.* 138, 62–69. doi: 10.1016/j.jaap.2018.12.007

Chen, H., Ferrari, C., Angiuli, M., Yao, J., Raspi, C., and Bramanti, E. (2010). Qualitative and quantitative analysis of wood samples by Fourier transform infrared spectroscopy and multivariate analysis. *Carbohydr. Polym.* 82, 772–778. doi: 10.1016/j.carbpol.2010.05.052

Chen, G.-B., Li, Y.-H., Chen, G.-L., and Wu, W.-T. (2017). Effects of catalysts on pyrolysis of castor meal. *Energy* 119, 1–9. doi: 10.1016/j.energy.2016.12.070

Czernik, S., Johnson, D. K., and Black, S. (1994). Stability of wood fast pyrolysis oil. *Biomass Bioenergy* 7, 187–192. doi: 10.1016/0961-9534(94)00058-2

Dalluge, D. L., Whitmer, L. E., Polin, J. P., Choi, Y. S., Shanks, B. H., and Brown, R. C. (2019). Comparison of direct and indirect contact heat exchange to improve recovery of bio-oil. *Appl. Energy* 251, 113346. doi: 10.1016/j.apenergy.2019.113346

Dickerson, T., and Soria, J. (2013). Catalytic fast pyrolysis: a review. *Energies* 6, 514–538. doi: 10.3390/en6010514

Diebold, J. P., and Czernik, S. (1997). Additives to lower and stabilize the viscosity of pyrolysis oils during storage. *Energy Fuels* 11, 1081–1091. doi: 10.1021/ef9700339

Du, S., Sun, Y., Gamliel, D. P., Valla, J. A., and Bollas, G. M. (2014). Catalytic pyrolysis of miscanthus×giganteus in a spouted bed reactor. *Biores. Technol.* 169, 188–197. doi: 10.1016/j.biortech.2014.06.104

Dufour, A., Girods, P., Masson, E., Normand, S., Rogaume, Y., and Zoulalian, A. (2007). Comparison of two methods of measuring wood pyrolysis tar. *J. Chromatogr. A* 1164, 240–247. doi: 10.1016/j.chroma.2007.06.049

Easterly, J. L. (2002). Assessment of bio-oil as a replacement for heating oil. *Northeast Region. Biomass Program* 1, 1–15.

Ellens, C. J., and Brown, R. C. (2012). Optimization of a free-fall reactor for the production of fast pyrolysis bio-oil. *Biores. Technol.* 103, 374–380. doi: 10.1016/j.biortech.2011.09.087

Elliott, D. C., Oasmaa, A., Preto, F., Meier, D., and Bridgwater, A. V. (2012). Results of the IEA round robin on viscosity and stability of fast pyrolysis bio-oils. *Energy Fuels* 26, 3769–3776. doi: 10.1021/ef300384t

Faix, O. (1992). "Fourier Transform Infrared Spectroscopy," in *Methods in Lignin Chemistry*. Eds. S. Y. Lin and C. W. Dence (Heidelberg: Springer, Berlin), 83–109. doi: 10.1007/978-3-642-74065-7_7

Faix, O., Fortmann, I., Bremer, J., and Meier, D. (1991). Thermal degradation products of wood. A collection of electron-impact (EI) mass spectra of polysaccharide derived products. *Holz als Roh- und Werkstoff (Germany F.R.).* 49, 299–304. doi: 10.1007/BF02663795

Faix, O., Meier, D., and Fortmann, I. (1990a). Gas chromatographic separation and mass spectrometric characterization of monomeric lignin derived products. *Holz als roh-und werkstoff* 48, 281–285. doi: 10.1007/BF02626519

Faix, O., Meier, D., and Fortmann, I. (1990b). Thermal degradation products of wood. A collection of electron-impact (EI) mass spectra of monomeric lignin derived products. *Holz als Roh- und Werkstoff* 48, 351–354. doi: 10.1007/BF02639897

Fermoso, J., Pizarro, P., Coronado, J. M., and Serrano, D. P. (2017). Advanced biofuels production by upgrading of pyrolysis bio-oil. *WIREs Energy Environ.* 6, e245. doi: 10.1002/wene.245

Ghorbannezhad, P., Park, S., and Onwudili, J. A. (2020). Co-pyrolysis of biomass and plastic waste over zeolite- and sodium-based catalysts for enhanced yields of hydrocarbon products. *Waste Manage.* 102, 909–918. doi: 10.1016/j.wasman.2019.12.006

Grioui, N., Halouani, K., and Agblevor, F. A. (2014). Bio-oil from pyrolysis of Tunisian almond shell: Comparative study and investigation of aging effect during long storage. *Energy Sustain. Dev.* 21, 100–112. doi: 10.1016/j.esd.2014.05.006

Gupta, S., and Mondal, P. (2021). Catalytic pyrolysis of pine needles with nickel doped gamma-alumina: Reaction kinetics, mechanism, thermodynamics and products analysis. *J. Clean. Product.* 286, 124930. doi: 10.1016/j.jclepro.2020.124930

Harman-Ware, E., Orton, K., Deng, C., Kenrick, S., Carpenter, D., and Ferrell, J. (2020). Molecular weight distribution of raw and catalytic fast pyrolysis oils: comparison of analytical methodologies. *RSC Adv.* 10, 3789–3795. doi: 10.1039/C9RA09726K

Hassan, E. M., Steele, P. H., and Ingram, L. (2009). Characterization of fast pyrolysis bio-oils produced from pretreated pine wood. *Appl. Biochem. Biotechnol.* 154, 3–13. doi: 10.1007/s12010-008-8445-3

Hita, I., Arandes, J. M., and Bilbao, J. (2020). "Upgrading of Bio-oil via Fluid Catalytic Cracking," in *Chemical Catalysts for Biomass Upgrading* (Hoboken, New Jersey, U.S: John Wiley & Sons, Ltd), 61–96. doi: 10.1002/9783527814794.ch3

Horne, P. A., Nugranad, N., and Williams, P. T. (1995). Catalytic coprocessing of biomass-derived pyrolysis vapours and methanol. *J. Anal. Appl. Pyrol.* 34, 87–108. doi: 10.1016/0165-2370(94)00877-4

Hu, B., Lu, Q., Jiang, X., Liu, J., Cui, M., Dong, C., et al. (2019). Formation mechanism of hydroxyacetone in glucose pyrolysis: A combined experimental and theoretical study. *Proc. Combustion Instit.* 37, 2741–2748. doi: 10.1016/j.proci.2018.05.146

Hu, B., Zhang, Z., Xie, W., Liu, J., Li, Y., Zhang, W., et al. (2022). Advances on the fast pyrolysis of biomass for the selective preparation of phenolic compounds. *Fuel Process. Technol.* 237, 107465. doi: 10.1016/j.fuproc.2022.107465

Imran, A., Bramer, E. A., Seshan, K., and Brem, G. (2018). An overview of catalysts in biomass pyrolysis for production of biofuels. *Biofuel Research Journal.* 5, 872–885. doi: 10.18331/BRJ2018.5.4.2

Isahak, W. N. R. W., Hisham, M. W., Yarmo, M. A., and Hin, T. Y. (2012). A review on bio-oil production from biomass by using pyrolysis method. *Renewable Sustain. Energy Rev.* 16, 5910–5923. doi: 10.1016/j.rser.2012.05.039

Jacobson, K., Maheria, K. C., and Kumar Dalai, A. (2013). Bio-oil valorization: A review. *Renewable Sustain. Energy Rev.* 23, 91–106. doi: 10.1016/j.rser.2013.02.036

Jarvis, J. M., McKenna, A. M., Hilten, R. N., Das, K. C., Rodgers, R. P., and Marshall, A. G. (2012). Characterization of pine pellet and peanut hull pyrolysis bio-oils by negative-ion electrospray ionization fourier transform ion cyclotron resonance mass spectrometry. *Energy Fuels* 26, 3810–3815. doi: 10.1021/ef300385f

Jia, L. Y., Raad, M., Hamieh, S., Toufaily, J., Hamieh, T., Bettahar, M., et al. (2017). Catalytic fast pyrolysis of biomass: superior selectivity of hierarchical zeolites to aromatics. *Green Chem.* 19, 5442–5459. doi: 10.1039/C7GC02309J

Junming, X., Jianchun, J., Yunjuan, S., and Yanju, L. (2008). Bio-oil upgrading by means of ethyl ester production in reactive distillation to remove water and to improve storage and fuel characteristics. *Biomass Bioenergy* 32, 1056–1061. doi: 10.1016/j.biombioe.2008.02.002

Kang, B.-S., Lee, K. H., Park, H. J., Park, Y.-K., and Kim, J.-S. (2006). Fast pyrolysis of radiata pine in a bench scale plant with a fluidized bed: Influence of a char separation system and reaction conditions on the production of bio-oil. *J. Anal. Appl. Pyrol.* 76, 32–37. doi: 10.1016/j.jaap.2005.06.012

Khuenkaeo, N., and Tippayawong, N. (2020). Production and characterization of bio-oil and biochar from ablative pyrolysis of lignocellulosic biomass residues. *Chem. Eng. Commun.* 207, 153–160. doi: 10.1080/00986445.2019.1574769

Kim, J.-S. (2015). Production, separation and applications of phenolic-rich bio-oil – A review. *Biores. Technol.* 178, 90–98. doi: 10.1016/j.biortech.2014.08.121

Kim, J.-S., and Park, K.-B. (2020). "Production of Phenols by Lignocellulosic Biomass Pyrolysis," in *Production of Biofuels and Chemicals with Pyrolysis*. Eds. Z. Fang, R. L. Smith Jr. and L. Xu (Springer, Singapore), 289–319. doi: 10.1007/978-981-15-2732-6_11

Le, D. M., Nielsen, A. D., Sørensen, H. R., and Meyer, A. S. (2017). Characterisation of authentic lignin biorefinery samples by fourier transform infrared spectroscopy and determination of the chemical formula for lignin. *Bioenerg. Res.* 10, 1025–1035. doi: 10.1007/s12155-017-9861-4

Lehto, J. (2007). Determination of kinetic parameters for Finnish milled peat using drop tube reactor and optical measurement techniques. *Fuel* 86, 1656–1663. doi: 10.1016/j.fuel.2006.12.020

Li, B., Ou, L., Dang, Q., Meyer, P., Jones, S., Brown, R., et al. (2015). Techno-economic and uncertainty analysis of *in situ* and *ex situ* fast pyrolysis for biofuel production. *Biores. Technol.* 196, 49–56. doi: 10.1016/j.biortech.2015.07.073

Li, S., Xu, S., Liu, S., Yang, C., and Lu, Q. (2004). Fast pyrolysis of biomass in free-fall reactor for hydrogen-rich gas. *Fuel Process. Technol.* 85, 1201–1211. doi: 10.1016/j.fuproc.2003.11.043

Liu, Y., Lotero, E., and Goodwin, J. G. (2006). A comparison of the esterification of acetic acid with methanol using heterogeneous versus homogeneous acid catalysis. *J. Catal.* 242, 278–286. doi: 10.1016/j.jcat.2006.05.026

Liu, Y., Shi, Q., Zhang, Y., He, Y., Chung, K. H., Zhao, S., et al. (2012). Characterization of red pine pyrolysis bio-oil by gas chromatography–mass spectrometry and negative-ion electrospray ionization fourier transform ion cyclotron resonance mass spectrometry. *Energy Fuels* 26, 4532–4539. doi: 10.1021/ef300501t

Luo, G., and Resende, F. L. P. (2016). *In-situ* and *ex-situ* upgrading of pyrolysis vapors from beetle-killed trees. *Fuel* 166, 367–375. doi: 10.1016/j.fuel.2015.10.126

Lyu, G., Wu, S., and Zhang, H. (2015). Estimation and comparison of bio-oil components from different pyrolysis conditions. *Front. Energy Res.* 3. doi: 10.3389/fenrg.2015.00028

Mahfud, F. H., Melián-Cabrera, I., Manurung, R., and Heeres, H. J. (2007). Biomass to fuels: upgrading of flash pyrolysis oil by reactive distillation using a high boiling alcohol and acid catalysts. *Process Saf. Environ. Prot.* 85, 466–472. doi: 10.1205/psep07013

Mantilla, S. V., Manrique, A. M., and Gauthier-Maradei, P. (2015). Methodology for extraction of phenolic compounds of bio-oil from agricultural biomass wastes. *Waste Biomass Valor* 6, 371–383. doi: 10.1007/s12649-015-9361-8

Matsuoka, K., Shinbori, T., Kuramoto, K., Nanba, T., Morita, A., Hatano, H., et al. (2006). Mechanism of woody biomass pyrolysis and gasification in a fluidized bed of porous alumina particles. *Energy Fuels* 20, 1315–1320. doi: 10.1021/ef0600210

Miettinen, I., Kuittinen, S., Paasikallio, V., Mäkinen, M., Pappinen, A., and Jänis, J. (2017). Characterization of fast pyrolysis oil from short-rotation willow by high-resolution Fourier transform ion cyclotron resonance mass spectrometry. *Fuel* 207, 189–197. doi: 10.1016/j.fuel.2017.06.053

Miettinen, I., Mäkinen, M., Vilppo, T., and Jänis, J. (2015). Compositional characterization of phase-separated pine wood slow pyrolysis oil by negative-ion electrospray ionization fourier transform ion cyclotron resonance mass spectrometry. *Energy Fuels* 29, 1758–1765. doi: 10.1021/ef5025966

Mirkouei, A., Haapala, K. R., Sessions, J., and Murthy, G. S. (2017). A mixed biomass-based energy supply chain for enhancing economic and environmental sustainability benefits: A multi-criteria decision making framework. *Appl. Energy* 206, 1088–1101. doi: 10.1016/j.apenergy.2017.09.001

Mirkouei, A., Mirzaie, P., Haapala, K. R., Sessions, J., and Murthy, G. S. (2016). Reducing the cost and environmental impact of integrated fixed and mobile bio-oil refinery supply chains. *J. clean. product.* 113, 495–507. doi: 10.1016/j.jclepro.2015.11.023

Mosallanejad, S., Dlugogorski, B. Z., Kennedy, E. M., and Stockenhuber, M. (2018). On the chemistry of iron oxide supported on γ-alumina and silica catalysts. *ACS Omega* 3, 5362–5374. doi: 10.1021/acsomega.8b00201

Myllyviita, T., Holma, A., Antikainen, R., Lähtinen, K., and Leskinen, P. (2012). Assessing environmental impacts of biomass production chains – application of life cycle assessment (LCA) and multi-criteria decision analysis (MCDA). *J. Clean. Product.* 29–30, 238–245. doi: 10.1016/j.jclepro.2012.01.019

Ngo, T.-A., and Kim, J. (2014). Fast pyrolysis of pine wood chip in a free fall reactor: the effect of pyrolysis temperature and sweep gas flow rate. *Energy Sourc. Part A: Recov. Util. Environ. Effects* 36, 1158–1165. doi: 10.1080/15567036.2011.631089

Oasmaa, A., and Czernik, S. (1999). Fuel oil quality of biomass pyrolysis oils-state of the art for the end users. *Energy Fuels* 13, 914–921. doi: 10.1021/ef980272b

Oasmaa, A., and Kuoppala, E. (2003). Fast pyrolysis of forestry residue. 3. Storage stability of liquid fuel. *Energy Fuels* 17, 1075–1084. doi: 10.1021/ef030011o

Oasmaa, A., Kuoppala, E., Selin, J.-F., Gust, S., and Solantausta, Y. (2004). Fast pyrolysis of forestry residue and pine. 4. Improvement of the product quality by solvent addition. *Energy Fuels* 18, 1578–1583. doi: 10.1021/ef040038n

Papari, S., and Hawboldt, K. (2018). A review on condensing system for biomass pyrolysis process. *Fuel Process. Technol.* 180, 1–13. doi: 10.1016/j.fuproc.2018.08.001

Park, H. C., Choi, H. S., and Lee, J. E. (2016). Heat transfer of bio-oil in a direct contact heat exchanger during condensation. *Korean J. Chem. Eng.* 33, 1159–1169. doi: 10.1007/s11814-015-0256-y

Pattiya, A., Sukkasi, S., and Goodwin, V. (2012). Fast pyrolysis of sugarcane and cassava residues in a free-fall reactor. *Energy* 44, 1067–1077. doi: 10.1016/j.energy.2012.04.035

Pham, T. N., Sooknoi, T., Crossley, S. P., and Resasco, D. E. (2013). Ketonization of carboxylic acids: mechanisms, catalysts, and implications for biomass conversion. *ACS Catal.* 3, 2456–2473. doi: 10.1021/cs400501h

Poletto, M. (2018). "Lignin: Trends and Applications," in *BoD – Books on Demand*. (Janeza Trdine 9,51000 Rijeka, Croatia: Intech). doi: 10.5772/intechopen.68464

Punsuwan, N., and Tangsathitkulchai, C. (2014). Product characterization and kinetics of biomass pyrolysis in a three-zone free-fall reactor. *Int. J. Chem. Eng.* 2014, e986719. doi: 10.1155/2014/986719

Quirino, R. L., Tavares, A. P., Peres, A. C., Rubim, J. C., and Suarez, P. A. Z. (2009). Studying the influence of alumina catalysts doped with tin and zinc oxides in the soybean oil pyrolysis reaction. *J. Am. Oil Chem. Soc.* 86, 167–172. doi: 10.1007/s11746-008-1331-x

Ramirez-Corredores, M. M., and Sanchez, V. (2012). Challenges on the quality of biomass derived products for bringing them into the fuels market. *J. Energy Power Eng.* 6, 321–328.

Sotoudehnia, F., Baba Rabiu, A., Alayat, A., and McDonald, A. G. (2020). Characterization of bio-oil and biochar from pyrolysis of waste corrugated cardboard. *J. Anal. Appl. Pyrol.* 145, 104722. doi: 10.1016/j.jaap.2019.104722

Sotoudehnia, F., Orji, B., Mengistie, E., Alayat, A. M., and McDonald, A. G. (2021). Catalytic upgrading of pyrolysis wax oil obtained from waxed corrugated cardboard using zeolite Y catalyst. *Energy Fuels* 35, 9450–9461. doi: 10.1021/acs.energyfuels.1c00767

Sotoudehniakarani, F., Alayat, A., and McDonald, A. G. (2019). Characterization and comparison of pyrolysis products from fast pyrolysis of commercial Chlorella vulgaris and cultivated microalgae. *J. Anal. Appl. Pyrol.* 139, 258–273. doi: 10.1016/j.jaap.2019.02.014

Struhs, E., Sotoudehnia, F., Mirkouei, A., McDonald, A. G., and Ramirez-Corredores, M. M. (2022). Effect of feedstocks and free-fall pyrolysis on bio-oil and biochar attributes. *J. Anal. Appl. Pyrol.* 166, 105616. doi: 10.1016/j.jaap.2022.105616

Trueba, M., and Trasatti, S. P. (2005). γ-alumina as a support for catalysts: A review of fundamental aspects. *Eur. J. Inorg. Chem.* 2005, 3393–3403. doi: 10.1002/ejic.200500348

Tsai, W. T., Lee, M. K., and Chang, Y. M. (2006). Fast pyrolysis of rice straw, sugarcane bagasse and coconut shell in an induction-heating reactor. *J. Anal. Appl. Pyrol.* 76, 230–237. doi: 10.1016/j.jaap.2005.11.007

U.S. Department of Energy, Idaho National Laboratory (2016). *Bioenergy Feedstock Library*. Available online at: https://bioenergylibrary.inl.gov/Home/Home.aspx (Accessed January 25, 2022).

U.S. DOE Energy Information Administration (2023). *Monthly Energy Review - August 2023*. Available online at: http://www.eia.gov/totalenergy/data/monthly/pdf/mer.pdf.

Vasalos, I. A., Lappas, A. A., Kopalidou, E. P., and Kalogiannis, K. G. (2016). Biomass catalytic pyrolysis: process design and economic analysis. *WIREs Energy Environ.* 5, 370–383. doi: 10.1002/wene.192

Venderbosch, R. H. (2015). A critical view on catalytic pyrolysis of biomass. *ChemSusChem* 8, 1306–1316. doi: 10.1002/cssc.201500115

Wang, K., Johnston, P. A., and Brown, R. C. (2014). Comparison of *in-situ* and *ex-situ* catalytic pyrolysis in a micro-reactor system. *Biores. Technol.* 173, 124–131. doi: 10.1016/j.biortech.2014.09.097

Wenting, F., Ronghou, L., Weiqi, Z., Yuanfei, M., and Renzhan, Y. (2014). Influence of methanol additive on bio-oil stability. *Int. J. Agric. Biol. Eng.* 7, 83–92. doi: 10.25165/ijabe.v7i3.986

Xu, F., Wang, B., Yang, D., Ming, X., Jiang, Y., Hao, J., et al. (2018). TG-FTIR and Py-GC/MS study on pyrolysis mechanism and products distribution of waste bicycle tire. *Energy Conver. Manage.* 175, 288–297. doi: 10.1016/j.enconman.2018.09.013

Xu, F., Xu, Y., Lu, R., Sheng, G.-P., and Yu, H.-Q. (2011). Elucidation of the thermal deterioration mechanism of bio-oil pyrolyzed from rice husk using fourier transform infrared spectroscopy. *J. Agric. Food Chem.* 59, 9243–9249. doi: 10.1021/jf202198u

Yang, Z., Kumar, A., and Huhnke, R. L. (2015). Review of recent developments to improve storage and transportation stability of bio-oil. *Renewable Sustain. Energy Rev.* 50, 859–870. doi: 10.1016/j.rser.2015.05.025

Zhang, L., Bao, Z., Xia, S., Lu, Q., and Walters, K. (2018). Catalytic pyrolysis of biomass and polymer wastes. *Catalysts* 8, 659. doi: 10.3390/catal8120659

Zhang, Q., Chang, J., Wang, T., and Xu, Y. (2007). Review of biomass pyrolysis oil properties and upgrading research. *Energy Conver. Manage.* 48, 87–92. doi: 10.1016/j.enconman.2006.05.010

Zhang, Q., Chang, J., and Xu, Y. (2006). Upgrading bio-oil over different solid catalysts. *Energy Fuels* 20, 2717–2720. doi: 10.1021/ef060224o

Zhang, J., Jiang, Y., F. Easterling, L., Anstner, A., Li, W., Z. Alzarieni, K., et al. (2021). Compositional analysis of organosolv poplar lignin by using high-performance liquid chromatography/high-resolution multi-stage tandem mass spectrometry. *Green Chem.* 23, 983–1000. doi: 10.1039/D0GC03398G

Zhang, J., Sekyere, D. T., Niwamanya, N., Huang, Y., Barigye, A., and Tian, Y. (2022). Study on the staged and direct fast pyrolysis behavior of waste pine sawdust using high heating rate TG-FTIR and Py-GC/MS. *ACS Omega* 7, 4245–4256. doi: 10.1021/acsomega.1c05907

Zhang, M., and Wu, H. (2014). Phase behavior and fuel properties of bio-oil/glycerol/methanol blends. *Energy Fuels* 28, 4650–4656. doi: 10.1021/ef501176z